Appendixes 2: Extraction of Profile Information from Cloud Contaminated Radiances

Extraction of Profile Information from Cloud Contaminated Radiances

W. L. Smith, D. K. Zhou[1], H-L Huang[2], Jun Li[2], X. Liu[1], and A. M. Larar[1]

[1] NASA Langley Research Center, Hampton VA
[2] UW-CIMSS, Madison WI
bill.l.smith@cox.net

1. Introduction

Clouds act to reduce the signal level and may produce noise dependence on the complexity of the cloud properties and the manner in which they are treated in the profile retrieval process. There are essentially three ways to extract profile information from cloud contaminated radiances: (1) cloud-clearing using spatially adjacent cloud contaminated radiance measurements, (2) retrieval based upon the assumption of opaque cloud conditions, and (3) retrieval or radiance assimilation using a physically correct cloud radiative transfer model which accounts for the absorption and scattering of the radiance observed. Cloud clearing extracts the radiance arising from the clear air portion of partly clouded fields of view permitting soundings to the surface or the assimilation of radiances as in the clear field of view case. However, the accuracy of the clear air radiance signal depends upon the cloud height and optical property uniformity across the two fields of view used in the cloud clearing process. The assumption of opaque clouds within the field of view permits relatively accurate profiles to be retrieved down to near cloud top levels, the accuracy near the cloud top level being dependent upon the actual microphysical properties of the cloud. The use of a physically correct cloud radiative transfer model enables accurate retrievals down to cloud top levels and below semi-transparent cloud layers (e.g., cirrus). It should also be possible to assimilate cloudy radiances directly into the model given a physically correct cloud radiative transfer model using geometric and microphysical cloud parameters retrieved from the radiance spectra as initial cloud variables in the radiance assimilation process. This presentation reviews the above three ways to extract profile information from cloud-contaminated radiances. NPOESS Airborne Sounder Testbed-Interferometer (Smith et. al., 1999) radiance spectra and Aqua satellite AIRS (Aumann et. al., 2003) radiance spectra are used to illustrate how cloudy radiances can be used in the profile retrieval process.

2. Cloud Handling Techniques

The vertical resolution of soundings obtained from high spectral resolution infrared spectrometers is highly dependent on the radiance signal to noise ratio. Clouds act to reduce the signal level and may produce noise dependent on the complexity of the cloud properties and the manner in which they are treated in the profile retrieval process. There are essentially four ways used to deal with clouds: (a) hole hunting, (b) cloud-clearing using spatially adjacent radiance measurements, (c) opaque cloud training, and (d) realistic cloud training.

(a) Hole hunting: The success of hole hunting is highly dependent upon the instrument field of view size. Figure 1 below shows that for the field of view size of the current and planned polar orbiting sounding instruments (i.e., AIRS, IASI, and CrIS), the percentage of 50 km x 50 km sounding regions with clear fields of view will be too small (i.e., < 30 %) to provide adequate global sounding coverage. Thus, we must be able to treat clouds in either the sounding retrieval or the radiance assimilation process in order to get the full value of these data in global numerical weather prediction.

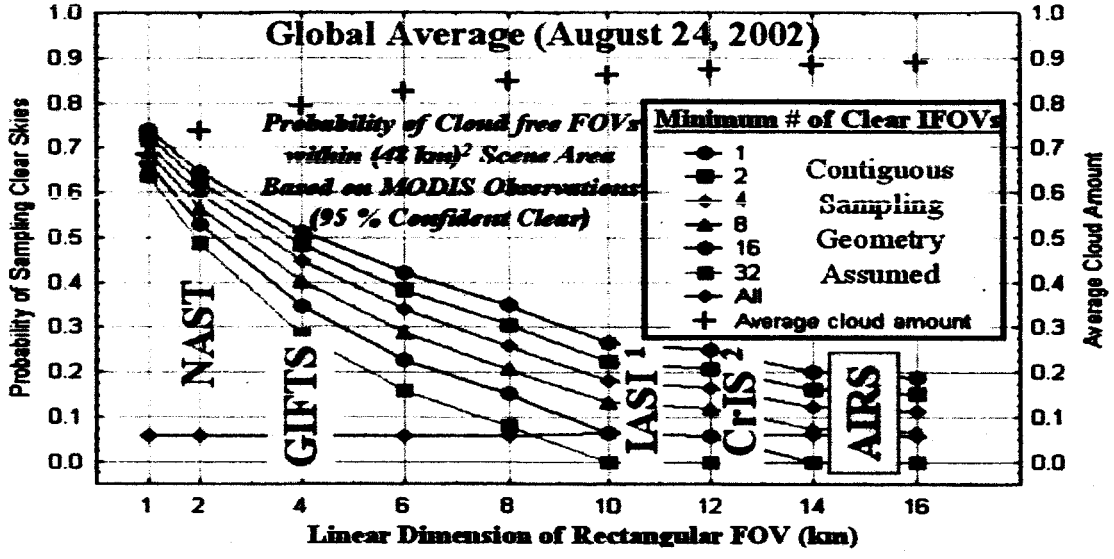

[1]IASI is circular with a diameter of 12 km, [2] CrIS is circular with a diameter of 14 km

Figure 1: Probability of sampling clear air as a function of field of view size

(b) Cloud clearing: Cloud clearing produces the radiance observed in the clear air portion of a partly cloudy area, and therefore soundings to the surface, when the cloud height and optical properties are horizontally uniform (Smith, 1968). Figure 2 below shows a cloud-clearing algorithm formulated for utilizing high spatial resolution imager observations (i.e., MODIS) for processing the low spectral resolution Aqua AIRS spectral radiance data. As can be seen, under the assumption of horizontally uniform surface and atmospheric condition, including cloud height and cloud microphysical properties, the radiance for the clear portion of a set of partly cloudy fields of view can be extracted from the cloud contaminated radiances given a single parameter, N*. Since N* is independent of spectral frequency, it can be defined from the observed radiances for a single spectral channel whose radiance is heavily influenced by the cloud, provided that the clear radiance for that channel is known. N* can thus be defined by using the clear air radiances observed within the two adjacent sounding instrument fields of view as observed with a high spatial resolution imager together with the cloud contaminated radiances observed with the sounding instrument. In this case the radiances for an atmospheric window spectral region (i.e., 10.5 – 11.5 micron) are used for both instruments. The high spectral resolution radiances from the sounding instrument are spectrally convoluted using the instrument response function of the lower spectral, but higher spatial, resolution imaging radiometer for the determination of N*. Once N* is defined, the clear air spectrum for the sounding instrument can be calculated as shown in

figure 2. Other imager instrument clear air spectral channel radiances can then be approximated by spectral convolutions of the derived sounder clear air spectrum. A comparison of the sounder simulated clear air radiances for the imaging instrument spectral channels with those actually observed by the imager enables erroneous estimates arising from non-uniform surface and atmospheric conditions to be filtered from the set to be used for atmospheric sounding determination or for direct assimilation into the NWP model analysis/prediction process.

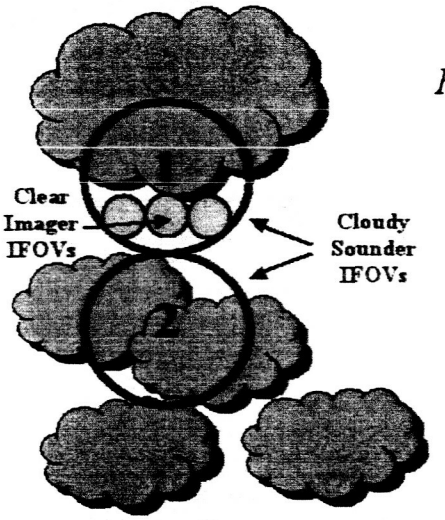

$$R_{clr}(\nu) = \frac{R_1(\nu) - N^*(\nu) R_2(\nu)}{1 - N^*(\nu)}$$

where $N^*(\nu) = \varepsilon(\nu)_1 N_1 / \varepsilon_2(\nu) N_2$.

$$N^*(W) = \frac{R_1(W) - \overline{R}_{clr}(\Delta W)}{R_2(W) - \overline{R}_{clr}(\Delta W)}$$

$$\hat{R}_{clr}(\Delta\nu) = \int \theta(\nu) R_{clr}(\nu) d\nu$$

Filter:

$$\left| \hat{R}_{clr}(\Delta\nu) - R_{clr}(\Delta\nu) \right| \geq \delta$$

$R_1(W)$ and $R_2(W)$ are sounder window radiance measurements in FOVs 1 and 2. $R_{clr}(\Delta W)$ is the clear window radiance measured by the imager. $R_{clr}(\Delta\nu)$ is the clear radiance measured in the absorption channel(s) of the imager. δ is the expected error, due to measurement noise, between the true and reconstructed imager clear radiances.

Figure 2: Basic cloud clearing methodology. The relationships are valid under the assumption of horizontally uniform cloud height and microphysical properties.

For the case of the Aqua satellite, the MODIS imaging spectrometer possesses numerous 1 km spatial resolution spectral absorption channels, which overlap the spectral coverage of the AIRS (see figure 3 below).

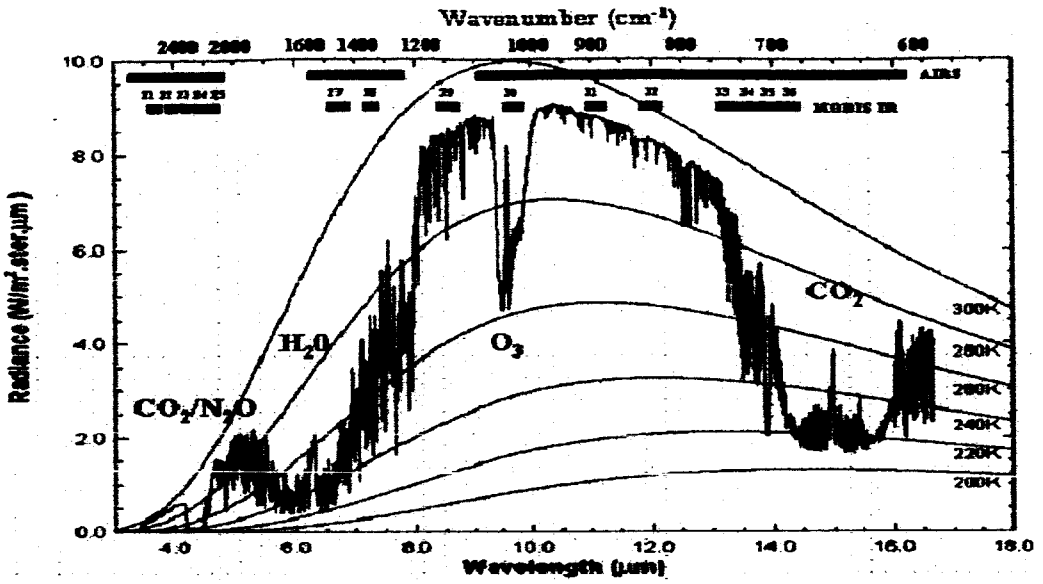

Figure 3: MODIS spectral channels (green) and AIRS spectral coverage (red).

An example of the extraction of the clear air radiance from a set of cloud-contaminated fields of view is shown in figure 4. Here the derived clear air spectrum is compared with a nearby observed clear sky spectrum. The derivation is for radiances observed over water and for low-level scattered cumulus cloud conditions. As can be seen, the clear air spectrum is successfully determined for this case.

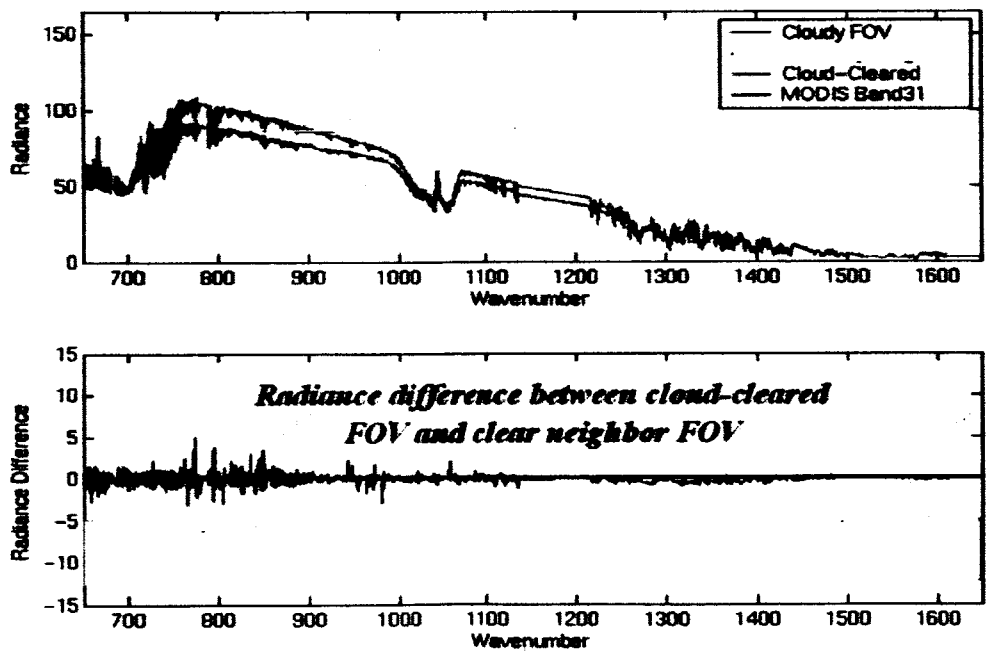

Figure 4: Example clear air radiance spectrum derived from the combination of Aqua AIRS and MODIS data

Table 1 below shows the clear air sounding radiance yields without and with the use of MODIS absorption channel data for filtering erroneous cloud cleared radiance spectra.

Here, the radiance spectra, for different spatial resolutions, and MODIS observations were simulated from NPOESS Airborne Sounder Testbed Interferometer (NAST-I) data, which have a 3 km spatial resolution (Smith et. al., 2003). Only cases where at least one clear NAST-I field of view within the 40 km x 40 km sounding area were included in the analysis since for these cases the correct clear radiance spectrum was known for validation purposes. The spatial resolution most representative of the AIRS is the 18 km linear resolution case. As shown, the yields of the MODIS absorption channel filtered data are only slightly lower than the unfiltered data indicating that the high N* filter (**i.e., N* > 0.75**) was able to detect many of the erroneous cloud cleared radiance estimates.

Table 1: 40 km x 40 km Sounding Area Clear Field of View Radiance Yields (%)

Spatial Resolution	3km	6km	9km	12 km	18 km
Total Number of FOVs/ FOR	144	36	16	9	4
≥ 1 Observed Clear FOV/FOR (%)	46	40	33	28	21
Total (Clr + CCR) w/o MODIS (%)	66	62	56	53	45
Total with MODIS (%)	**64**	**58**	**52**	**47**	**39**

However, as shown in figure 5 below, there is a significant difference in the accuracy between the error estimates for these two cases. Without the use of the MODIS filter, the errors of the clear sky estimates are too large to be useful for retrieval or radiance assimilation. With the use of MODIS, more acceptable results are achieved but these errors are still larger than those desired for the extraction of profile information with high vertical resolution.

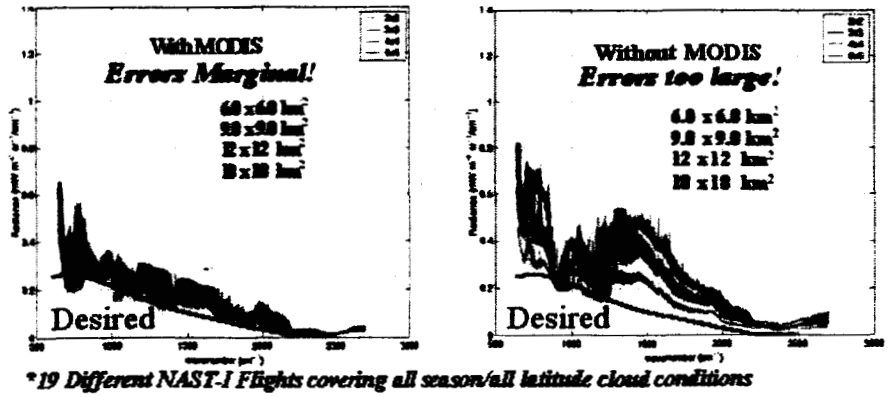

**19 Different NAST-I Flights covering all season/all latitude cloud conditions*

Figure 5: Cloud clearing with and without imager absorption channels (i.e., MODIS).

(c) Opaque cloud assumption: Assuming that opaque clouds exist within the instruments field of view produces, accurate profiles can be retrieved down to levels

close to the cloud top level. This is because there is an ambiguity between an opaque cloud condition and a clear atmospheric profile, which is isothermal below the cloud level. The vertical resolution of the hyperspectral radiance measurements is high enough to resolve the equivalent isothermal condition within 1-2 km of the cloud level. Thus merely treating an opaque cloud radiance spectrum as if it were from a clear sky atmospheric condition should tend to result in the retrieval of the correct atmospheric profile above the cloud top level, with a fictitious isothermal, and saturated, profile condition being retrieved below the cloud top level. The retrieved relative humidity and the abrupt change in vertical temperature lapse rate enable one to determine the cloud level.

Figure 6 below shows an example of results assuming clear atmospheric conditions for cloud-contaminated radiances as observed with the NAST-I instrument. Here the retrieval method is the Eigenvector (EOF) regression method (Smith and Woolf, 1976, and Zhou et. al., 2002) where training data set, used for the radiative transfer calculations, included cloudy radiosondes in which the temperature profile was adjusted to be isothermal, and the relative humidity was set to 100 %, below the cloud level (Smith et al., 2004). Thus, the regression relations were trained to retrieve the clear sky equivalent profiles below the cloud under cloudy sky conditions. As can be seen, under the clear sky assumption, the temperature tends toward the isothermal condition and the relative humidity tends toward saturation to a degree dependent upon the opacity of the cloud. Even in the clear air columns between the cloud elements, where the temperature profile does not tend towards the isothermal condition, the layer of high moisture responsible for the existence of the nearby clouds can be seen in the relative humidity vertical structure. The advantage of this simple approach for handling clouds is that it allows profile information down to cloud level to be assimilated into the model. However, it is not clear how to incorporate this information for the case where one is assimilating radiances rather than retrievals. One method might be to replace the erroneous profile retrieved below the cloud top level with the model profile and recompute the radiances using the hybrid profiles. The radiances whose weighting functions peak at and above the cloud level, which are heavily influenced by the retrieved profiles above cloud level, can then be assimilated as clear air radiances.

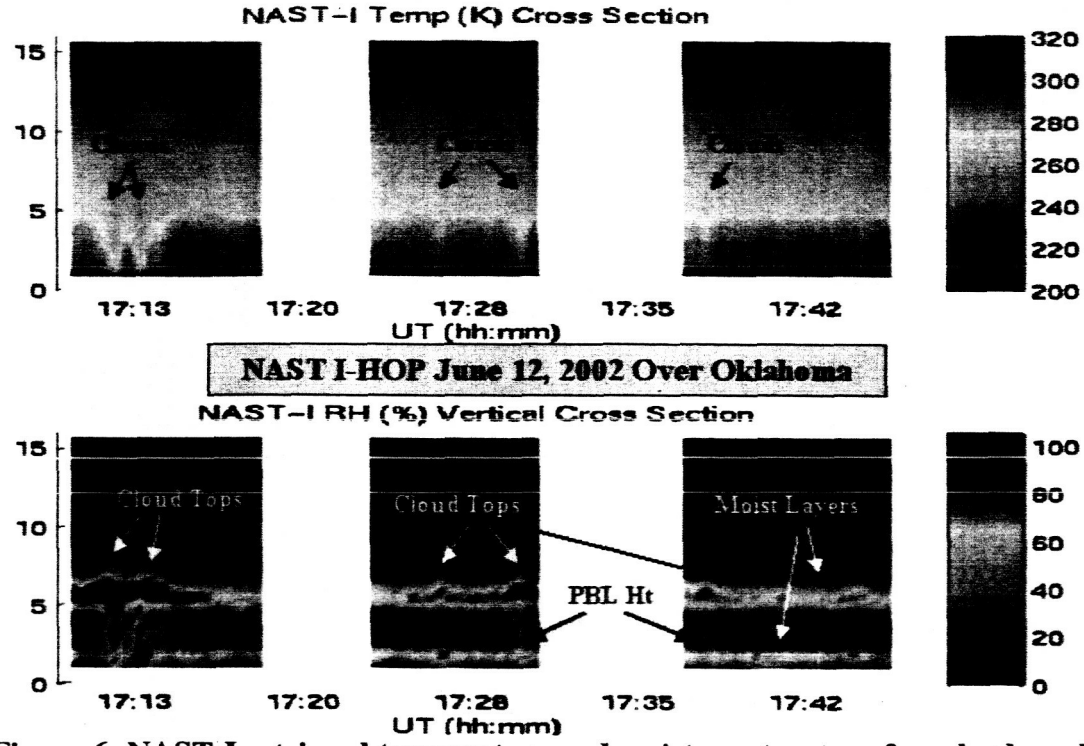

Figure 6: NAST-I retrieved temperature and moisture structure for a broken cloud condition with cloud tops near the 6 km level.

(d) Realistic Cloud Radiative Transfer Model: However, if the clouds are high and there is significant spectral structure in the absorption of the clouds (i.e., a common characteristic of Cirrus clouds), errors in the profiles above the clouds may occur. Thus for high cloud cases, a more realistic cloud model is required to get accurate profiles down to the cloud top level. Also, if the cloud is semi-transparent or broken, the profile below the cloud level should be retrievable using a physically based cloud radiative transfer model. The physically based cloud radiative transfer model was developed by the University of Wisconsin – CIMSS (Huang et. al., 2004) using DISORT calculations performed for a wide variety of cloud microphysical properties by Ping Yang, at the Texas A&M University (Yang et. al., 2003). For the retrieval using the EOF regression method, the clouds can now be included in a more realistic manner with a statistical distribution in accordance with real observations conducted over many years from aircraft and balloon (Heymsfeld et al., 2003). Table 2 below summarizes the characteristics of the realistic cloud model and the simulations of clouds as used for the EOF regression training. For semitransparent and/or scattered cloud with an effective optical depth (defined here as the exponential of a negative argument which is the product of the fractional cloud amount times the cloud visible optical depth), which is less than unity, the correct profile below the cloud is attempted to be retrieved. If a lower level cloud underlies the semitransparent and/or scattered upper level cloud, the lower level cloud is treated as an equivalent clear isothermal condition as described above for the opaque cloud condition retrieval. EOF regression enables both the cloud height and the cloud microphysical properties of the highest-level cloud to be estimated.

Table 2: Cloud Radiative Transfer Model and Cloud Simulation Characteristics

- **Perform a realistic simulation of clouds for synthetic EOF radiance training**
- **Diagnose 0-2 cloud layers from radiosonde relative humidity profile**
  - A single cloud layer (either ice or liquid) is inserted into the input radiosonde profile.
  - Approximate lower level cloud using opaque cloud representation (i.e., isothermal/saturated)
- **Use parameterization of Heymsfeld's* balloon and aircraft cloud microphysical data base (2003) to specify cloud effective particle radius, r_e, and cloud optical depth, τ, (i.e., $r_e = a\,\tau^c / [\tau - b\tau^c]$) .**
  - Different habitats can be specified (Hexagonal columns assumed here)
  - Different clouds microphysical properties are simulated for same radiosonde using random number generator to specify visible cloud optical depth within a pre-specified range. 10 % random error added to parameterized effective radius to account for real data scatter.
- **Use LBLRTM/DISORT "lookup table" to specify cloud radiative properties**
  - Spectral transmittance and reflectance for ice and liquid clouds interpolated from multi-dimensional look-up table based on DISORT multiple scattering calculations for the (wavenumber range 500 – 2500 cm^{-1}, zenith angle 0 – 80 deg., Deff (Ice: 10 – 157 um, Liquid: 2 – 100 um), OD(vis) (Ice: 0.04 - 100, Liquid 0.06 – 150)
- **Compute EOFs and Regressions from cloudy radiance data base**
  - Regress cloud properties (p, τ, r_e) and surface and profile parameters against radiance EOFs
  - For small optical depth, output entire profile down to surface or lower opaque cloud level
  - For large upper level cloud optical depth, output profile above the upper cloud level

Heymsfield, A. J., S. Matrosov, and B. A. Baum: Ice water path-optical depth relationships for cirrus and precipitating cloud layers. *J. Appl. Meteor.* October 2003

Figure 7 shows a vertical cross section of temperature and moisture profiles retrieved from NASA ER-2 aircraft NAST-I data for a very cloudy situation. The retrieved cloud height is compared with that estimated from a nadir looking Cloud Physics LIDAR (CPL) on-board the ER-2 aircraft. The flight track is shown over visible and IR images from the GOES spacecraft. A comparison of a NAST-I profile at 19 GMT with the 00 GMT MHX radiosonde is also shown alongside cross-section near the radiosonde station. The retrievals were produced using the EOF regression method where a very large sample of radiosondes from a ten year period was used to simulate NAST radiances. Clouds were introduced at levels where the radiosonde humidity exceeded a threshold prescribed as a function of altitude. Cloud microphysical properties were assigned using a random number generator to define an optical depth between 0 and 4, from a uniform distribution of the logarithm of the optical depth, and the effective particle radius was defined using the relation provided in table 2 above which is based on many years of cloud microphysical property observations from balloon and aircraft. The particle radius is changed by a random amount selected from a guassian distribution of random numbers with a standard deviation of 10% in order to represent the scatter of real observations. If two or more cloud layers exist, the lower level clouds are represented as a the equivalent cloudfree isothermal temperature condition in the radiative transfer calculation. Thus the attempt is to retrieve profiles below optically thin upper level cloud only (e.g., thin Cirrus). Regression relations are also generated for predicting cloud height, visible optical depth, and particle diameter. Because the radiance is highly non-linear with respect to cloud height, statistics are formulated for one class of data which contains all cloud height conditions and eight other height classes for which the cloud height has been stratified to within 1 km of the mean for that class. The final cloud height class to be used for the retrievals is obtained by iteration beginning with the unclassified class to predict the initial cloud height stratification for the retrievals. Usually, the final cloud height class is defined within five iterations of the cloud height prediction process.

In the retrievals shown in figure 7, the profiles retrieved below clouds with a predicted optical depth greater than 1 were considered missing since their accuracy would be degraded from that achievable under cloudless sky conditions.

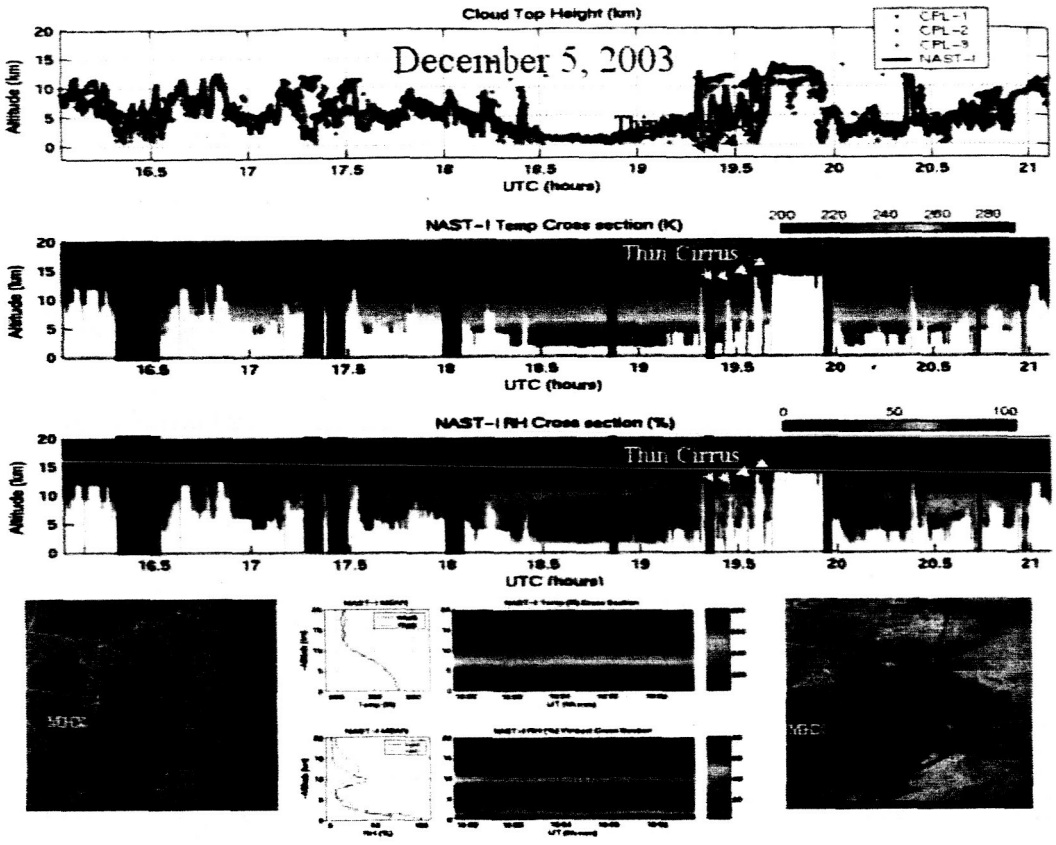

Figure 7: Temperature and humidity cross-sections from NAST-I cloud contaminated radiances observed along the flight track of the NASA ER-2 aircraft flying at 20km flight altitude over a wide variety of clouds.

As can be seen there is excellent agreement between the LIDAR and NAST-I retrieved cloud heights indicating that the retrieval of other properties, such as the cloud microphysical properties and the temperature and humidity profiles should also be accurate. The horizontal uniformity of the retrieved temperature and humidity conditions across the wide variety of cloud height conditions indicate that this is the case.

Evidence of the accuracy of the profile conditions which can be retrieved under cloud conditions is given by figure 8 which shows a comparison of the EOF regression retrievals for this case obtained from AIRS and NAST-I data in comparison to dropsonde observations made along the flight track of the ER-2. One can see excellent correspondence between all three observations even though their time differences may be as large as 4 hours.

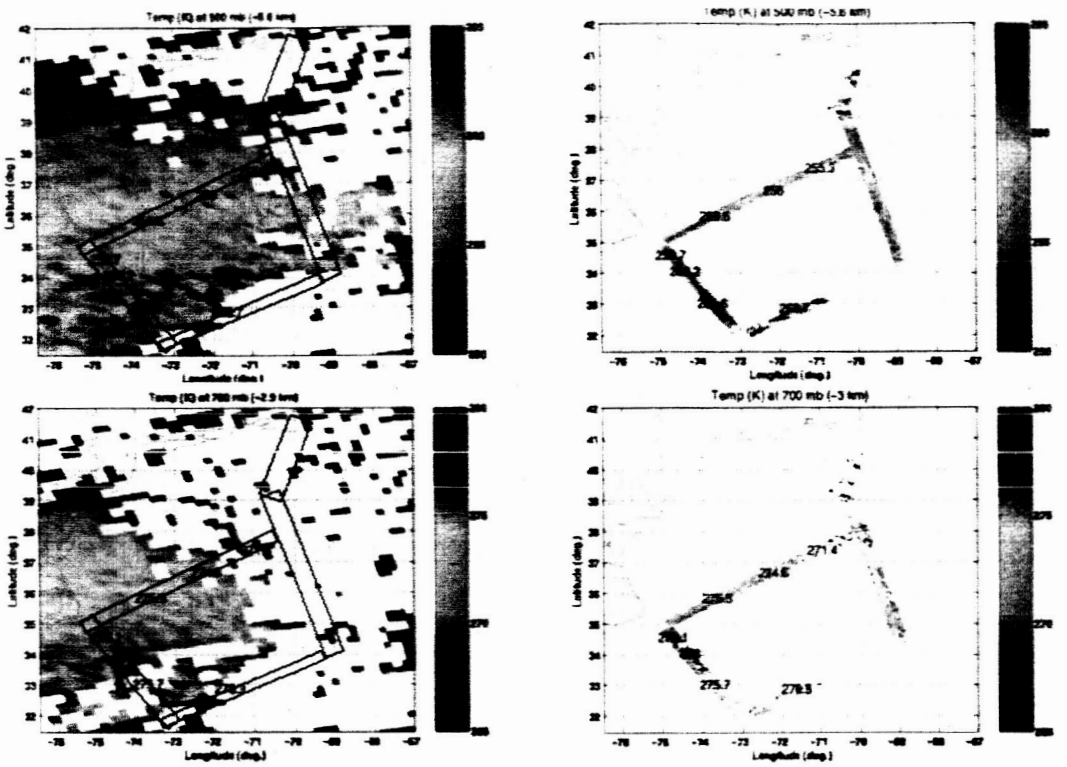

Figure 8: Retrievals of atmospheric temperature at 500mb and 700 MB obtained from Aqua satellite AIRS radiance spectra and NAST-I radiance spectra. Dropsondes from the NOAA Gulfstream along the track of the ER-2 aircraft are shown to validate the retrieval results.

For the radiance assimilation process, one might use the retrieved cloud height, optical depth, and particle diameter properties with the cloud radiative transfer model used here in the assimilation process. Spectral radiances for channels which peak below clouds with an optical depth greater than unity could be deleted from the assimilation process in order to minimize the effects of errors in the cloud representation.

3. Summary and Conclusions

Cloud greatly complicates the interpretation of infrared sounding data. The new hyperspectral resolution infrared sounding systems alleviate much of the ambiguity between cloud and atmospheric temperature and moisture contributions. However, in heavily clouded situations, the thermodynamic profile information to be retrieved is limited to the atmosphere above clouds. The results of the study presented here indicate some success in the ability to retrieve information below scattered and partially transparent Cirrus cloud (i.e., clouds with effective optical depths of less than unity). The thermodynamic profile information can be obtained by a combination of cloud clearing and by direct retrieval from the clouded radiances using a realistic cloud radiative transfer model. Results achieved with airborne NAST-I and Aqua satellite NAST-I observations show that accuracies close to those achieved in totally cloud-free conditions can be achieved down to cloud top levels. The accuracy of the profile retrieved below cloud top level is dependent upon the optical depth and fractional coverage of the cloud.

For the assimilation of cloudy radiances into an NWP model, two approaches might be considered: (1) an indirect method whereby clear sky equivalent radiances are assimilated, and (2) a direct method in which the actual cloud radiances are assimilated. For the indirect method, a combined EOF regression retrieval followed by a 1-d variational retrieval, using the cloud parameters from the EOF regression retrieval, is performed and the results above the highest cloud level with an effective optical depth greater than one is amalgamated with the model profile to recompute the equivalent clear sky radiances for the hybrid

atmospheric profile condition. One can then assimilate the "clear" radiance whose weighting functions peak above the derived cloud level.

In the direct cloudy radiance assimilation method, a cloudy sky condition radiative transfer model is used in the assimilation process. In this technique the intial cloud parameters for the radiative transfer calculation are taken from the EOF regression retrieval. The cloud parameters are allowed to adjust as part of the cloudy radiance assimilation process.

The implementation of either of the two approaches suggested above requires a considerable research development effort. However, cloudy sky radiative transfer models now exist which should enable the extraction of profile information from cloud contaminated radiances suitable for the numerical weather prediction application..

4. References

Aumann, Hartmut H.; Chahine, Moustafa T.; Gautier, Catherine; Goldberg, Mitchell D.; Kalnay, Eugenia; McMillin, Larry M.; Revercomb, Hank; Rosenkranz, Philip W.; Smith, William L.; Staelin, David H.; Strow, L. Larrabee, and Susskind, Joel. AIRS/AMSU/HSB on the Aqua Mission: Design, science objectives, data products, and processing systems. IEEE Transactions on Geoscience and Remote Sensing v.41, no.2, 2003, pp253-264.

Cousins, D., and W. L. Smith, 1997: National Polar-Orbiting Operational Environmental Satellite System (NPOESS) Airborne Sounder Testbed-Interferometer (NAST-I), in *Proceedings, SPIE Application of Lidar to Current Atmospheric Topics II*, A. J. Sedlacek, and K. W. Fischer, eds., 3127, 323–331.

Heymsfield, Andrew J.; Matrosov, Sergey, and Baum, Bryan. "Ice water path-optical depth relationship for cirrus and deep stratoform cirrus cloud layers". Journal of Applied Meteorology v.42 , no.10, 2003, pp1369-1390. Re

Huang, Hung-Lung; Tobin, Dave; Li, Jun; Olson, Erik; Baggett, Kevin; Huang, Bormin; Mecikalski, John; Knuteson, Bob; Osborne, Brian; Posselt, Derek; Antonelli, Paolo; Revercomb, Hank ; Smith, William, and Yang, Ping. "Hyperspectral radiance simulator - cloud radiance modeling and beyond". Optical Remote Sensing of the Atmosphere and Clouds III, Hangzhou, China, 25-27 October 2002. Bellingham, WA, International Society for Optical Engineering, (SPIE), 2003, pp180-189. Reprint #3477.

Liu, X., J.-L. Moncet, D. K. Zhou, and W. L. Smith, 2003: A Fast and Accurate Forward Model for NAST-I Instrument, *Fourier Transform Spectroscopy and Optical Remote Sensing of Atmosphere, OSA Topical Meetings,* Feb. 2003, Quebec, Canada.

Smith, W.L., 1968: And improved method for calculating tropospheric temperature and moisture from satellite radiometer measurements. *Mon. Wea. Rev.*, 96, 387-396.

Smith, W. L., and H. M. Woolf, 1976: The use of eigenvectors of statistical co-variance matrices for interpreting satellite sounding radiometer observations, *J. Atmos. Sci.*, 33, 1,127–1,140.

Smith, W. L., A. M. Larar, D. K. Zhou, C. A. Sisko, J. Li, B. Huang, H. B. Howell, H. E. Revercomb, D. Cousins, M. J. Gazarik, D. Mooney, 1999: NAST-I: results from revolutionary aircraft sounding spectrometer, in *Proceedings, SPIE Optical* A. M. Larar, ed., 3756, 2–8.

Smith, W. L., G. E. Bingham, G. W. Cantwell, M. J. Gordon, D. K. Zhou, and H-L. Huang, "AIRS Cloud-clearing Using Multi-spectral MODIS Imagery", Available from **bill.l.smith@larc.nasa.gov**

Smith, W. L., D. K. Zhou, A. M. Larar, S. A. Mango, H. B. Howell, R. O. Knuteson, H. E. Revercomb, and W. L. Smith Jr " The NPOESS Airborne Sounding Testbed Interferometer - Remotely Sensed Surface and Atmospheric Conditions during CLAMS", accepted fopr publication on the Journal of the Atmospheric Sciences, Special Issue: "Chesapeake Lighthouse and Aircraft Measurements for Satellites (CLAMS) Field Experiment", 2004

Yang P., B. C. Gao, B. A. Baum, Y. Hu, W. Wiscombe, S.-C. Tsay, D. M. Winker, S. L. Nasiri, 2001: Radiative Properties of cirrus clouds in the infrared (8-13 um) spectral region, *J. Quant. Spectros. Radiat. Transfer*, 70, 473-504.

Yang P., B.-C. Gao, W. Wiscombe, M. I. Mishchenko, S. Platnick, H.-L. Huang, B. A. Baum, Y. X. Hu, D. Winker, S.-C. Tsay, and S. K. Park, 2002: Inherent and apparent scattering properties of coated or uncoated spheres embedded in an absorbing host medium. Appl. Opt. 41, 2740-2759.

Yang, Ping; Wei, Heli; Kattawar, George W.; Hu, Yong X.; Winker, David M.; Hostetler, Chris A., and Baum, Bryan A. "Sensitivity of the backscattering Mueller matrix to particle shape and thermodynamic phase". Applied Optics v.42, no.21, 2003, pp4389-4395. Reprint #3557.

Zhou, D. K., W. L. Smith, J. Li, H. B. Howell, G. W. Cantwell, A. M. Larar, R. O. Knuteson, D. C. Tobin, H. E. Revercomb, and S. A. Mango, 2002: Thermodynamic product retrieval methodology for NAST-I and validation, *Applied Optics*, 41, 6,957–6,967.